Advanced Concepts for Ultra-Wide-Swath SAR Imaging

G. Krieger, N. Gebert, M. Younis, F. Bordoni, A. Patyuchenko, A. Moreira
Microwaves and Radar Institute, German Aerospace Center (DLR), Germany

***Abstract*— This paper reviews advanced multi-channel SAR system concepts for the imaging of ultra-wide swaths with high azimuth resolution. Novel system architectures and operational modes are introduced and compared to each other with regard to their performance.**

I. Introduction

Wide unambiguous swath coverage and high azimuth resolution pose contradicting requirements on the design of spaceborne SAR systems. To overcome this inherent limitation, several innovative techniques have been suggested where the receiving antenna is split into multiple sub-apertures that are connected to individual receiver channels (Fig. 1). The digitally recorded sub-aperture signals are combined in a spatiotemporal processor to simultaneously form multiple independent beams and to gather additional information about the direction of the scattered radar echoes. This information can be used to (1) suppress spatially ambiguous signal returns from the ground by null-steering, (2) increase the receiving gain without a reduction of the imaged area by switching between narrow, high gain beams, (3) suppress spatially localized interferences by space-time adaptive processing, and (4) gain additional information about the dynamic behaviour of the scatterers and their surroundings.

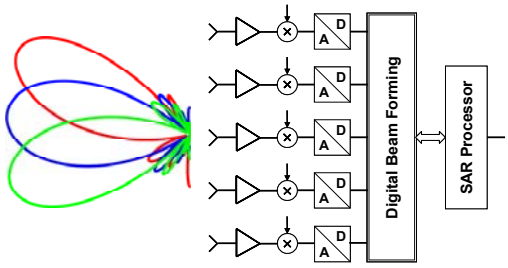

Fig. 1: Schematic of a multi-channel receiver. The signal from each sub-aperture element is independently amplified, down-converted, and digitized. The digital processing enables flexible and adaptive beamforming a posteriori to signal reception.

II. Advanced Multi-Channel SAR Architectures

A promising example for an advanced multi-channel SAR system is the High-Resolution Wide-Swath (HRWS) SAR which combines a fixed wide-area illuminator with a multi-aperture receiver array as illustrated in Fig. 2 on the left [1]. Each element of the receiver antenna is connected to an individual receiver channel. Multiple displaced apertures in along-track acquire additional samples along the synthetic aperture and enable thereby an efficient suppression of azimuth ambiguities [2][3][4]. Multiple channels in elevation improve the SNR without reducing the swath width by steering a highly directive receiver beam in real time such that it follows the radar pulse as it travels on the ground [1]. More advanced multi-channel SAR architectures, which avoid the use of separate Tx and Rx antennas, have been discussed in [5]. These architectures exploit the whole Tx/Rx aperture of a direct radiating array to improve the SAR performance via a multidimensional encoding of the transmitted waveforms.

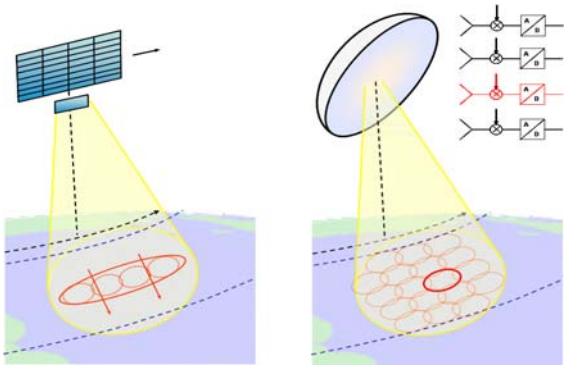

Fig. 2: Left: High-Resolution Wide-Swath (HRWS) SAR system employing direct radiating and receiving array antennas. Right: High-resolution wide-swath SAR employing a reflector antenna in combination with a digital feed array.

An interesting alternative to a planar array is a reflector antenna in combination with a digital feed array as illustrated schematically in Fig. 2 on the right. This architecture, which may be of special interest for low frequency radar systems operating in L- and P-band, combines the capabilities of digital beamforming with the high directivity of a large reflector antenna. The reflector could be deployable as suggested for several forthcoming radar missions. Unfurlable antennas are now a mature technology with extensive flight heritage in space telecommunications and lightweight mesh reflectors with diameters of 20 m and more will be deployed in space in the near future.

The reflector based architecture offers the potential to use all array elements simultaneously for the transmission of a broad beam without spill-over as desired for wide swath illumination. Alternatively, separate waveforms can be used for the individual feed array elements. This enables optimized modes employing multidimensional waveform encoding [6]. Individual transmission and recording from the feed elements can moreover measure and adaptively compensate signal deteriorations from reflector deformations via (ground reflected) calibration pulses.

For a paraboloidal reflector with a feed array close to the focal point, the signals from a given direction (or a small footprint as indicated by the small red ellipses in Fig. 2 on the right) correspond typically to only one or a small subset of activated feed elements. This beam direction to array element correspondence may be of advantage to reduce the implementation complexity and the costs of a digital beamforming radar. For example, if one wants to follow a radar pulse with a high gain beam as it travels on the ground, it is not necessary to implement the aforementioned real-time beamsteering involving a linear combination of all array elements, but it is sufficient to simply read out the signals from different feed array elements in successive order since only one or a small number of feed elements are activated above the noise level at each instant of time. The number of simultaneously activated feed elements depends on their distance from the focal point, i.e. more elements are activated as the scan-angle distance off the main beam axis in-

creases. The selection of active elements, which can also be regarded as a sparse coding that suppresses the noise from unused Rx-modules to improve the SNR, could be computed either a priori from geometric considerations or one may use appropriate thresholds to automatically route only a sparse subset of element signals, thereby avoiding the storage of irrelevant data[1] (see simplified sketches on the right hand side of Fig. 3). The sparse routing of the Rx feed element signals enables a much simpler, less power consuming, and more cost-effective implementation of a "digital beamforming SAR" which does not necessarily need (but would nevertheless benefit from) a sophisticated on-board multi-channel real-time processor.

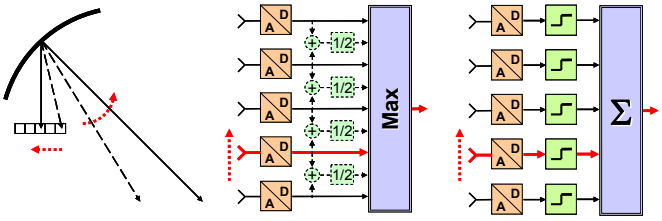

Fig. 3: The beam direction to feed element correspondence (left) enables implementations of digital beamforming with reduced complexity, e.g. via maximum selection (middle) or summation/routing of thresholded element signals (right).

III. Advanced Operational Modes

The previous section discussed different multi-channel architectures for future high-resolution wide-swath SAR systems. In the following, we introduce and compare different SAR imaging modes that take advantage from the new digital radar architectures. As a design example, we consider a system which enables a continuous coherent monitoring of the Earth with a weekly observation period. This requires at the equator a swath width of approx. 400 km. The azimuth resolution shall be 5 m. Such a system exceeds by far the capabilities for current spaceborne SAR sensors. To avoid too strong variations of the incident angle we assume an orbital altitude of 750 km.

A. Multi-Channel Stripmap Mode

We first consider a multi-aperture mapping in standard stripmap mode. The timing diagram in Fig. 4 reveals that the imaging of a contiguous 400 km swath from a 750 km orbit requires a PRF in the order of 400 Hz. The minimum and maximum incident angles are 24° and 48°, respectively. Assuming "full resolution" SAR imaging, the necessary antenna length to avoid azimuth ambiguities can be approximated by $l_{ant} \approx 2v/PRF$ which yields an antenna length of $l_{ant} \approx 35$ m. The achievable azimuth resolution is then in the order of $\Delta az \approx 20$ m. By illuminating a wider Doppler spectrum and dividing the receiver antenna into multiple azimuth apertures with individual receiver channels it becomes possible to improve the azimuth resolution to $\Delta az \approx l_{ant}/(2N_{az})$ where N_{az} is the number of independent azimuth channels. An azimuth resolution of 5 m hence requires at least N_{az}=4 channels. The resolution improvement without a rise of ambiguities is possible for both the direct radiating array and the reflector configuration. The performance gain can be understood in the former case as the acquisition of additional samples along the synthetic aperture and in the latter case as the acquisition of additional frequency sub-bands with different Doppler centroids to increase the overall azimuth bandwidth (Fig. 5).

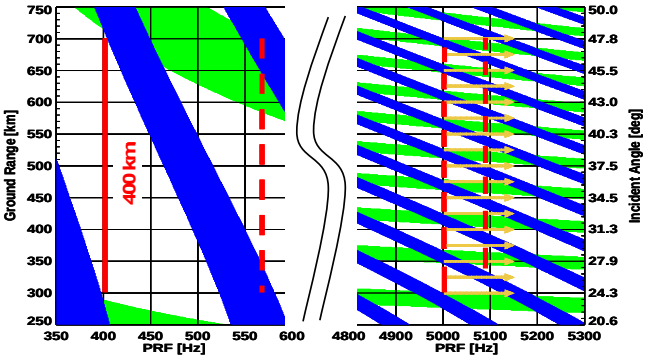

Fig. 4: Timing for h_{sat} = 750 km and a duty cycle of 16%.

Further demands arise for a fully polarimetric system where the transmit polarisation is toggled from pulse to pulse. An antenna length of $l_{ant} \approx 70$ m and $N_{az} = 8$ receiver channels are necessary to achieve the same swath width and azimuth resolution. To avoid this increase one may transmit the H and V polarisations via two contiguous sub-pulses as illustrated in Fig. 6. The sub-pulse echoes are separated by digital beamforming on receive in elevation which requires effective antenna heights[2] as shown in Fig. 7. Assuming a sub-pulse separation of $\Delta\tau_p$ = (0.16/2)/400 Hz = 200 µs, the antenna height is in the order of 1.3 m, 2.3 m, and 10 m for X-, C-, and L-band, respectively. The antenna dimensions can be reduced by multidimensional waveform encoding [5]. For example, a staggered illumination from far to near range allows for a shortened receiving window and therefore longer sub-pulse separations at higher incident angles. This enables in turn a reduction of the antenna height.

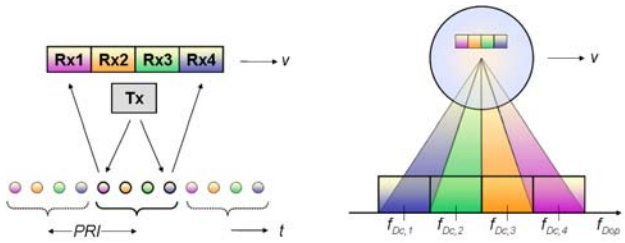

Fig. 5: Left: Multi-aperture receiver antenna for the acquisition of additional samples along the synthetic aperture. Right: Reflector antenna configuration with displaced feed elements for the simultaneous acquisition of multiple azimuth frequency sub-bands.

B. Multi-Channel ScanSAR Mode

Another possibility to map the 400 km swath is the ScanSAR (or TOPS) mode. Assuming an antenna length of 15 m the minimum PRF is in the order of 1 kHz. Timing considerations reveal that at least 4 bursts will be required to cover the 400 km swath. The azimuth resolution is then $\Delta az > (N_{burst}+1)\cdot l_{ant}/2 =$

[1] For long Tx chirp pulses, the activated element further depends on the instantaneous RF frequency, which requires either a frequency dependent selection or a summation among multiple feeds. A similar data compression strategy can be employed for planar direct radiating arrays if one performs first a spatial FFT among the simultaneously recorded array signals.

[2] The values in Fig. 7 are rough estimates for the height of a direct radiating array which allows steering a null to the ambiguous sub-pulse range while keeping the full gain for the desired sub-pulse echo. The diameter of a circular reflector should be correspondingly adapted.

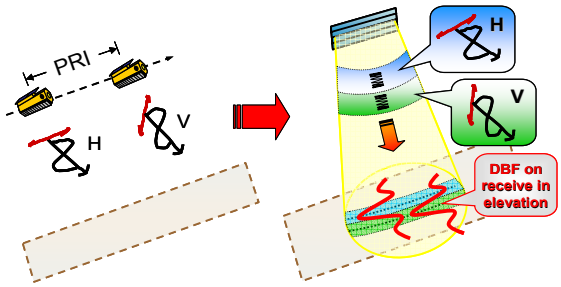

Fig. 6: Fully polarimetric waveform encoding

37.5 m. To achieve an azimuth resolution of Δaz = 5 m one may again employ multiple azimuth channels. The minimum number of required azimuth channels is $N_{az} > l_{ant}\cdot(N_{burst}+1)/(2\Delta az)$. Hence, at least 8 channels will be required. Further problems arise for the multi-aperture processing due to the varying target Doppler spectra together with the required variation of the PRFs [7]. The fully polarimetric mode necessitates additional azimuth channels in combination with either a longer antenna or additional bursts.

C. Multiple Beam ScanSAR Mode

The previous section revealed that the mapping of a wide image swath with a reasonable antenna length requires, especially in fully polarimetric mode, a large number of bursts. This impairs the performance and leads to conflicts with regard to the achievable azimuth resolution. Such problems can be mitigated by a simultaneous mapping of multiple swaths during each burst. The right hand side of Fig. 4 shows that two bursts with slightly different PRFs are sufficient to map an ultra-wide swath if it is possible to suppress nadir echoes by digital beamforming on receive. Here, a reflector antenna based digital beamforming receiver has the advantage to avoid possible saturation effects in the relevant receiver channels that could arise in case of very strong nadir returns. The strength of the nadir signal can in addition be reduced by a careful design of the Tx antenna pattern and a further improvement can be achieved by using different waveforms for each transmitted pulse which enables a spread of the nadir energy in the received echoes.

The two PRFs on the right hand side of Fig. 4 are sufficient to avoid azimuth ambiguities for a 3 m antenna length. It is hence possible to achieve the desired azimuth resolution of 5 m in a two burst operational mode with a single azimuth channel! The minimum antenna heights to separate the pulses from the different swaths are 1.3 m, 2.4 m, and 10 m for X-, C-, and L-band. Fully polarimetric operation requires either an increased PRF (and hence a higher antenna) or a doubling of both the number of azimuth channels and the Rx antenna length.

An inherent peculiarity of the multiple beam ScanSAR mode is the range varying azimuth resolution resulting from the constant burst length for all sub-swaths. A trivial solution to avoid this limitation is the acquisition of two sets of swaths with different PRFs in repeat passes. Hence, no burst-mode operation would be required, thereby improving the performance and simplifying the azimuth processing on the cost of a non-simultaneous imaging. Another opportunity is the use of additional PRFs or even a continuous variation of the PRF during the target exposure time. As an example one may consider a periodic PRF increase from 5000 Hz to 5150 Hz which shifts

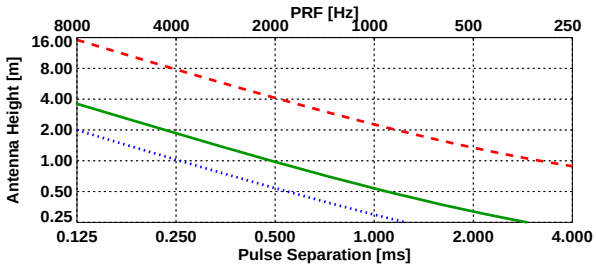

Fig. 7: Required antenna height for sub-pulse separation with digital beamforming on receive for X-band (dotted), C-band (solid), and L-band (dashed).

the blind ranges smoothly across the swath (cf. arrows on right hand side of Fig. 4). For each range one obtains then a contiguous burst of Tx pulses which is longer than in the two PRF case. The SAR focusing of the individual bursts requires a (rather simple) interpolation of the azimuth raw data to a uniform sampling interval. Another opportunity arises in case of extremely short transmit pulses [8]. Since one looses for each range only a very small segment of the synthetic aperture one may even consider a full interpolation in azimuth (cf. [9]).

D. Nonuniform Sampling

Another elegant solution to fill in the blind ranges has first been suggested in [10] and later independently rediscovered by DLR. The basic idea in [10] is to use a short repetitive sequence of transmit bursts with nonuniformly distributed inter-pulse time delays. This avoids the blind ranges for a wide range interval and one looses for each range only a small fraction of the transmitted pulses. The recorded azimuth signals are nonuniformly sampled and the SAR processing requires an adequate reconstruction algorithm. An alternative to the short recurrent pulse sequence is an optimized and slower variation of the pulse intervals that takes into account the travelling pulses in a spaceborne radar geometry. This optimization yields for each considered range an almost constant number of recorded pulses. By adapting the length of the whole sequence to the satellite height one could even ensure an overlap of the Tx events with the nadir returns. The optimization can moreover employ different pulse lengths, which allow also for a range-dependent distribution of the Tx power across the wide swath. Fig. 8 shows the azimuth sampling gaps for an exemplary Tx sequence with a non-uniform PRI variation between PRI_{min} = 0.25 ms and PRI_{max} = 0.375 ms. The maximum inter-pulse distance is below $2\cdot PRI_{max}$ = 0.75 ms for all considered ranges, since the optimization successfully avoided the loss of two consecutive pulses. The maximum sampling distance of 0.75 ms corresponds to a minimum PRF of 1.33 kHz and it is hence possible to avoid azimuth ambiguities with an antenna length of 11.3 m by a rather simple signal interpolation. Taking into account that

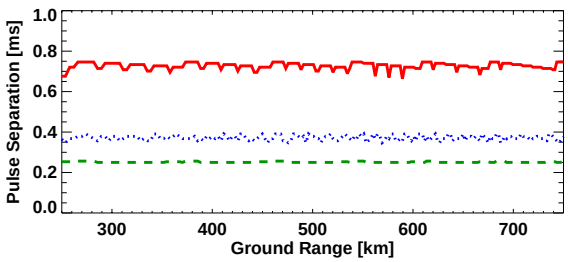

Fig. 8: Maximum (solid), mean (dotted), and minimum (dashed) separation of recorded pulses from nonuniform PRI transmission.

the mean Rx-PRI is below 0.4 ms, one can even reduce this antenna length below 10 m, which allows for an azimuth resolution of approx. 5 m without any scalloping deteriorations as in the previous burst mode systems. A further optimization could take into account that typically not the whole but only a part of the range chirp is blocked in the receiver. Each individual range frequency is hence sampled with a higher mean azimuth frequency than the mean PRI of Fig. 8. The minimum pulse separation in Fig. 8 is 0.25 ms and the suppression of range ambiguities by digital beamforming in elevation requires hence antenna heights of 1.1 m, 1.9 m, and 7.9 m for X-, C-, and L-band, respectively.

E. Bistatic Ultra-Wide Swath SAR

A completely different solution to the wide swath imaging problem is a bistatic SAR which employs different Tx and Rx antennas on spatially separated platforms. Since it is now possible to simultaneously transmit and receive radar pulses, restrictions from the timing can be avoided [11]. This requires a suppression of the direct signal from the transmitter to the receiver(s), e.g. via digital beamforming on receive and/or a narrow notch azimuth filter which removes the "DC" component from the (almost) constant Tx-Rx separation. Nadir echoes can again be suppressed by a combination of (1) appropriate Tx antenna pattern design, (2) digital beamforming on receive, (3) continuous PRF variation, (4) variation of the Tx waveform on a pulse-to-pulse level. The transmitter could moreover use an uninterrupted illumination like in a frequency modulated continuous waveform (FMCW) radar. This reduces the peak power requirements in the transmitter and lowers in the receiver(s) the amplitude of the interfering contributions from both the direct signal and the nadir echoes. Further opportunities for wide swath imaging have been discussed in [12].

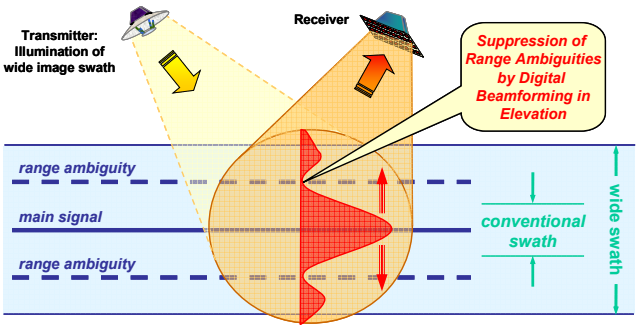

Fig. 9: Bistatic SAR for wide swath imaging employing a multi-channel digital beamforming receiver.

IV. Discussion

We have introduced several new SAR system concepts for the acquisition of high resolution radar images with ultra wide swath coverage. These innovative concepts rely on the combination of advanced multi-channel radar front-end architectures with novel operational modes. Table 1 compares the required antenna sizes for the different SAR imaging modes discussed in this paper. It becomes clear that the innovative modes enable the design of high-resolution ultra-wide-swath SAR sensors with rather compact antennas. The antenna dimensions can in principle be further reduced by employing multidimensional waveform encoding techniques as introduced in [5].

Operational Mode	Ant. Length	N_{az}	Antenna Height		
			L	C	X
DPCA Stripmap	35 m	4	1.2 m	0.3 m	0.2 m
DPCA Stripmap Quad	70 m	8	1.2 m	0.3 m	0.2 m
DPCA Strip. Quad + Sub-Pulse	35 m	4	10 m	2.3 m	1.3 m
DPCA Strip. Quad + Opt. Sub.	35 m	4	6 m	1.4 m	0.8 m
ScanSAR + DPCA (< 1.5 kHz)	15 m	8	3.2 m	0.8 m	0.5 m
Scan Quad + DPCA (< 3 kHz)	15 m	16	6 m	1.4 m	0.8 m
Multi-Beam 2 Burst (< 5.1 kHz)	3 m	1	10 m	2.4 m	1.3 m
Multi-Beam 2 Burst (< 2.6 kHz)	6 m	2	5.3 m	1.3 m	0.7 m
Multi-Beam 2 Burst Quad (5.1)	6 m	2	10 m	2.4 m	1.3 m
Multi-Beam 2 Burst Quad (2.6)	12 m	4	5.3 m	1.3 m	0.7 m
PRF Ramp (5 -5.15 kHz)	3 m	1	10 m	2.4 m	1.4 m
PRF Ramp (short duty + interp.)	10 m	1	3.5 m	0.9 m	0.5 m
PRF Ramp Quad (5 - 5.15 kHz)	6 m	2	10 m	2.4 m	1.4 m
PRF Ramp Quad (short duty)	10 m	1	6.5 m	1.6 m	0.9 m
Nonuniform PRI ($\Delta\tau$ > 0.25 ms)	< 10 m	1	7.9 m	1.9 m	1.1 m
Nonuniform PRI Quad (0.15 ms)	10 m	1	12.8 m	3.1 m	1.7 m
Bistatic (with short illuminator)	10 m	1	4.2 m	1.0 m	0.6 m
Bistatic (with long illuminator)	3 m	1	4.2 m	1.0 m	0.6 m
Bistatic Quad (short illuminator)	10 m	1	7.9 m	1.9 m	1.1 m
Bistatic Quad (long illuminator)	3 m	1	7.9 m	1.9 m	1.1 m

Table 1: Minimum antenna dimensions for imaging a 400 km swath with 5 m azimuth resolution. Values are for a planar array and represent first-order estimates to compare different operational modes.

Regarding implementation complexity, it was shown that deployable reflector antennas are an interesting alternative to direct radiating arrays and a low number of receiver channels are already sufficient to enhance the imaging capabilities far beyond those of current spaceborne SAR systems. The implementation of digital radar systems will moreover benefit from rapid developments in integrated microwaves and semi-conductor technologies [8]. For example, direct A/D conversion, which is already possible in L-band, simplifies the design of multi-channel receivers. In the long-term, one may even think about a multi-frequency SAR which employs the same digital receiver channels for different frequency bands. New semi-conductor technologies will furthermore pave the way to more advanced SAR systems with adaptive and hybrid imaging modes [5]. These sophisticated modes are well suited to resolve contradicting user requirements regarding resolution, coverage, and data acquisition continuity while taking into account limitations from both the available RF power and the downlink capacity.

V. References

[1] M. Suess, B. Grafmueller, R. Zahn, "A novel high resolution, wide swath SAR system," IGARSS'01, Sydney, Australia, pp. 1013-1015, 2001.

[2] A. Currie, M. A. Brown, "Wide-swath SAR," IEE Proceedings F - Radar and Signal Processing, vol. 139, pp. 122-135, 1992.

[3] G. Krieger, N. Gebert, A. Moreira, "Unambiguous SAR signal reconstruction from nonuniform displaced phase center sampling," IEEE Geoscience and Remote Sensing Letters, vol. 1, pp. 260-264, 2004.

[4] N. Gebert, G. Krieger, A. Moreira, "Digital beamforming on receive: techniques and optimization strategies for high-resolution wide-swath SAR imaging," IEEE Trans. Aerospace Electronic Systems, in print, 2008.

[5] G. Krieger, N. Gebert, A. Moreira, "Multidimensional waveform encoding: a new digital beamforming technique for radar remote sensing," IEEE Trans. Geoscience and Remote Sensing, vol. 46, no.1, pp. 31-46, 2008.

[6] G. Krieger, N. Gebert, M. Younis, A. Moreira, "Advanced Synthetic Aperture Radar Based on Digital Beamforming and Waveform Diversity", IEEE Radar Conf., 2008.

[7] N. Gebert, G. Krieger, A. Moreira, "Multi-channel ScanSAR for high-resolution ultra-wide-swath imaging", EUSAR 2008.

[8] M. Ludwig, M. Suess, N. Le Gallou, "Technologies for advanced SAR systems", EUSAR'06, Dresden, Germany, 2006.

[9] D. Salzman, R. Akamine, D Lefevre, JC Kirk, "Interrupted synthetic aperture radar (SAR)," IEEE AES Magazine, vol. 17, no. 5, pp. 33-39, 2002.

[10] B. Grafmüller, C. Schaefer, "Hochauflösende Synthetik-Apertur-Radarvorrichtung und Antenne", DE 10 2005 062 031.0 22.12.2005.

[11] G. Krieger, A. Moreira, "Potential of digital beamforming in bi- and multistatic SAR," IGARSS'03, Toulouse, France, pp. 527-529, 2003.

[12] G. Krieger, A. Moreira, "Spaceborne Bi- and Multistatic SAR: Potential and Challenges," IEE Proc. Radar, Sonar, Navigation, vol. 153, no. 3, pp. 184-198, 2006.